ACS Editors' Choice

JACS
JOURNAL OF THE AMERICAN CHEMICAL SOCIETY

Communication

pubs.acs.org/JACS

Terms of Use

β-NMR Measurements of Lithium Ion Transport in Thin Films of Pure and Lithium-Salt-Doped Poly(ethylene oxide)

Iain McKenzie,*[,†,‡] Masashi Harada,[§] Robert F. Kiefl,[†,∥] C. D. Philip Levy,[†] W. Andrew MacFarlane,[⊥] Gerald D. Morris,[†] Shin-Ichi Ogata,[§] Matthew R. Pearson,[†] and Jun Sugiyama[§]

[†]TRIUMF, Vancouver, B.C., Canada, V6T 2A3

[‡]Department of Chemistry, Simon Fraser University, Burnaby, B.C., Canada, V5A 1S6

[§]Toyota Central Research and Development Laboratories, Inc., Nagakute, Aichi 480-1192, Japan

[∥]Department of Physics and Astronomy, University of British Columbia, Vancouver, B.C., Canada, V6T 1Z1

[⊥]Department of Chemistry, University of British Columbia, Vancouver, B.C., Canada, V6T 1Z1

ABSTRACT: β-Detected nuclear spin relaxation of $^{8}Li^{+}$ has been used to study the microscopic diffusion of lithium ions in thin films of poly(ethylene oxide) (PEO), where the implanted lithium ions are present in extremely low concentration, and PEO with 30 wt % $LiCF_3SO_3$ over a wide range of temperatures both above and below the glass transition temperature. Recent measurements by Do et al. [*Phys. Rev. Lett.* **2013**, *111*, 018301] found that the temperature dependence of the Li^{+} conductivity was identical to that of the dielectric α relaxation and was well described by the Vogel−Fulcher−Tammann relation, implying the α relaxation dominates the Li^{+} transport process. In contrast, we find the hopping of Li^{+} in both samples in the high temperature viscoelastic phase follows an Arrhenius law and depends significantly on the salt content. We propose that the hopping of Li^{+} between cages involves motion of the polymer but that it is only for long-range diffusion where the α relaxation plays an important role.

Lithium-ion batteries are important to modern society due to their ubiquity in consumer products.[1] Their widespread use is due in part to their high energy density, absence of memory effects, and a slow loss of capacity.[2] Solid polymer electrolytes (SPEs) offer advantages over traditional ceramic and liquid electrolytes in that they are flexible, are moldable, and avoid the use of volatile solvents.[3] Poly(ethylene oxide) (PEO) is one of the most widely used SPEs due to its low glass transition temperature ($T_g \approx 215$ K), ability to dissolve high concentrations of salts, such as lithium triflate, $LiCF_3SO_3$, and ionic conductivities up to 10^{-4} S/cm.[4] Understanding the microscopic dynamics of lithium ions in a polymer matrix is crucial for optimizing SPEs for battery applications.

There have been numerous experimental and computational studies of PEO:salt solutions. Molecular dynamics (MD) simulations[5−7] suggest there are three different transport mechanisms: diffusion of Li^{+} along the chain, cooperative motion of Li^{+} with the chain, and Li^{+} transfer between different polymer chains. The Rouse-based models successfully reproduced the measured lithium self-diffusion coefficients.

NMR studies of PEO:$LiCF_3SO_3$ under conditions where the crystalline EO:Li = 3:1 complex and amorphous phase coexist demonstrate that ion transport occurs in the amorphous phase,[8] although Gadjourova et al. contend that ionic conductivity in the crystalline phase can be greater than in the amorphous material above T_g.[9] The temperature dependence of the ^{7}Li and ^{31}P line widths for crystalline PEO:$LiPF_6$ with EO:Li = 6:1 indicates ion transport in crystalline polymer electrolytes can be dominated by the motion of the cations, whereas both positive and negative ions are generally mobile in the amorphous phase. NMR experiments on PEO-based ionomers found that the motions of Li^{+} and the polymer backbone are strongly correlated in samples with low ion content.[10] The picture that has emerged from these measurements is that polymer motion plays a significant role in Li^{+} diffusion.

Do et al. recently studied PEO and PEO:LiTFSI (lithium bis(trifluoromethanesulfonyl)imide) with EO:Li = 10:1 using neutron scattering, dielectric spectroscopy, and MD simulations.[11] They found that both the α relaxation time and the DC resistivity follow the phenomenological Vogel−Fulcher−Tammann (VFT) equation with a Vogel−Fulcher temperature (T_{VF}) of 177 K. Dielectric measurements showed the β-relaxation in PEO:LiTFSI has an Arrhenius temperature dependence with an activation energy of 28 kJ/mol and the α and β processes merge just above room temperature. They concluded that the characteristic lifetime of Li^{+} within cages formed by several monomer units is mainly determined by the α-relaxation, which is associated with the segmental motion of the chain. The VFT dependence of Li^{+} conductivity in SPEs appears to be generally accepted.[12]

Do et al. noted that direct observation of cage trapping and hopping dynamics of Li^{+} cannot be easily studied and that improved knowledge of these processes would greatly improve our understanding of the Li^{+} transport mechanism. We have studied the microscopic Li^{+} dynamics in PEO and PEO with 30 wt % $LiCF_3SO_3$, which corresponds to EO:Li ≈ 8:1, using β-detected NMR (β-NMR) of implanted $^{8}Li^{+}$. β-NMR has been used to study the near-surface properties of magnetic systems,[13] superconductors,[14] and ion dynamics in solid systems[15] such as Li metal,[16] LiC_6,[17] LiAl,[18] and LiMg.[19] An advantage of β-NMR is that large concentrations of lithium salts are not needed, so we can study dynamics in both the Li^{+} concentrated and

Received: March 26, 2014
Published: May 25, 2014

   dx.doi.org/10.1021/ja503066a | *J. Am. Chem. Soc.* 2014, 136, 7833−7836

infinitely dilute limits to study the effect of the Li^+ concentration on cage trapping and hopping dynamics. The concentration of implanted $^8Li^+$ is extremely low, with a peak concentration of $\sim 5 \times 10^{-10}$ M.

The experiments were performed using the β-NMR spectrometer and $^8Li^+$ beam at the ISAC facility at TRIUMF. The spin-2 ^8Li nucleus has a lifetime of 1.2 s, gyromagnetic ratio of 630.15 Hz/G, and electric quadrupole moment of +31.4 mb. Nuclear spin polarization of ~70% was obtained by in-flight optical pumping. The 8 mm × 10 mm samples were mounted on a coldfinger cryostat in ultrahigh vacuum ($\sim 2 \times 10^{-10}$ Torr). The measurements were performed in a field of 6.55 T along the beam direction. This is significant as only fluctuations at the nuclear Larmor frequency $\nu_L = \gamma B \approx 41$ MHz are effective in relaxing the nuclear spin, setting the dynamic time scale sensed in the experiment.

The time dependence of the average ^8Li nuclear spin polarization is monitored through the β-decay asymmetry, which is given by $A(t) = [F(t) - B(t)]/[F(t) + B(t)]$, where $F(t)$ and $B(t)$ are the count rates in the forward and backward detectors, respectively. The time dependence of the polarization, $P(t)$, was modeled with a stretched exponential relaxation function:

$$P(t) = e^{-[(t-t_A)/T_1]^\beta} \quad (1)$$

where t_A is the arrival time of $^8Li^+$, T_1 is the spin−lattice relaxation time, and β is the stretching exponent. The normalized polarization is obtained by convoluting eq 1 with the square beam pulse.[20]

PEO was purchased from Sigma-Aldrich and had a M_W of 5×10^6 g/mol. Bulk T_g was determined to be 213 K, and the degree of crystallization is estimated to be 65% from DSC measurements. The ~200-nm-thick films were produced on epitaxially polished ⟨0001⟩ sapphire substrates (Crystal GMbH) by spin-coating following the procedure described by Mattsson et al.[21] Samples were annealed in vacuum at 330 K for ~48 h in order to remove any residual solvent and were then transferred to the spectrometer with minimal exposure to the atmosphere. Once mounted in the spectrometer, the samples were left in UHV at 317 K for several hours prior to starting the measurements.

The $^8Li^+$ ions were implanted at 6.9 keV, and the Stopping and Range of Ions in Matter (SRIM-2008.04[22]) code was used to calculate the initial stopping distribution. The mean initial depth was ~99 nm, and the range straggling was ~35 nm. The mobility of Li^+ can be so large that they will diffuse substantially during the 10-s observation window. Using parameters for the PEO:LiTFSI system[11] we estimate that the RMS displacement of Li^+ during the observation period is $\sim 7.5 \times 10^3$ nm at 300 K, which is much larger than the film thickness, and will be comparable to the film thickness around 260 K.

Examples of β-NMR spectra are shown in Figure 1, and the fitted values of $1/T_1$ and β are shown in Figure 2. The use of a stretched exponential is justified in disordered systems where there is a distribution of relaxation times, with the value of β reflecting the width of this distribution. Moreover, a modeling study by Borgs et al. of a lithium ion hopping between two sites with arbitrarily oriented local magnetic fields (that in our case would arise from dipolar fields of neighboring protons in PEO) found that the decay of the spin polarization is given by a stretched exponential.[23] The relaxation rate and β were found to depend on the Li^+ hop rate and the width of the internal

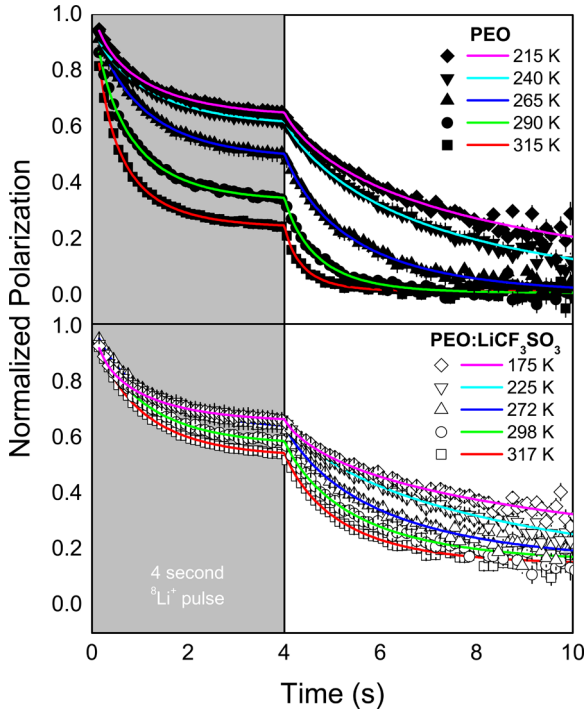

Figure 1. Nuclear spin relaxation of $^8Li^+$ at 6.55 T in PEO and PEO with 30 wt % $LiCF_3SO_3$. The solid lines are the fits using a stretched exponential model during both the 4 s ^8Li pulse (gray region) and the 6 s after the pulse.

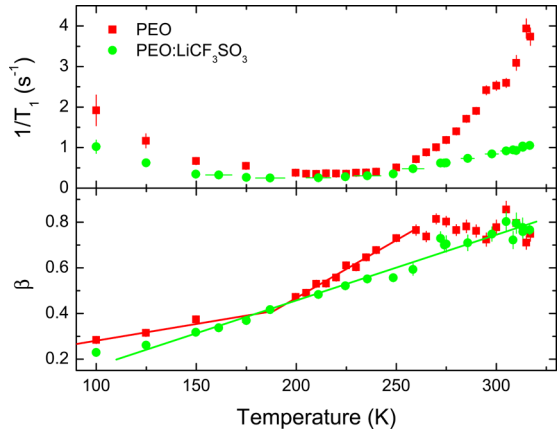

Figure 2. Temperature dependence of $1/T_1$ and β for PEO and PEO with 30 wt % $LiCF_3SO_3$. The lines are guides.

field distribution. We did not resolve distinct signals due to crystalline and amorphous regions and conclude that either the local hopping processes are of a similar magnitude in both regions or that the differences contribute to the value of β. For further analysis we consider the temperature dependence of the average relaxation time, $T_1^{avg} = (T_1/\beta)\Gamma(1/\beta)$, where Γ is the gamma function.

We assume the spin relaxation is primarily due to hopping of the Li^+, although polymer dynamics without Li^+ diffusion may contribute. Hopping between sites produces a fluctuating magnetic field at the ^8Li from the dipole−dipole interaction with nearby proton magnetic moments and also a fluctuating electric field gradient, which directly couples with the ^8Li spin.[24] We have used an expression for $1/T_1$ based on the

dx.doi.org/10.1021/ja503066a | J. Am. Chem. Soc. 2014, 136, 7833−7836

Bloembergen–Purcell–Pound (BPP) model[25] with modifications to account for a distribution of τ.[26]

$$\frac{1}{T_1} = K\left[\frac{\tau}{1 + (\omega_L\tau)^{1+\alpha}} + \frac{4\tau}{1 + (2\omega_L\tau)^{1+\alpha}}\right] \quad (2)$$

$\omega_L = 2\pi\nu_L$ is the Larmor frequency in radians per second, K is a constant that depends on the relaxation mechanism and spin quantum number, and α ranges from 0 to 1 (BPP).

Since we are looking at $1/T_1^{avg}$ we are concerned with an average hop rate of Li^+, which is assumed to follow Arrhenius behavior.

$$\tau^{-1} = \tau_0^{-1}\exp(-E_A/k_BT) \quad (3)$$

where E_A is the average activation energy, k_B is the Boltzmann constant, T is the temperature, and τ_0^{-1} is the pre-exponential factor, which is interpreted as the vibrational frequency of Li^+ in a potential well between hops and is $\sim 10^{12}$–10^{13} s^{-1}.[27] In the slow fluctuation limit, where $\omega_L\tau \gg 1$, the preceding equations can be combined to give

$$\ln(T_1/s) = -\ln\left[\frac{K'}{\omega_L^{1+\alpha}\tau_0^{\alpha}}\right] + \left(\frac{\alpha E_A}{k_B}\right)T^{-1} \quad (4)$$

In pure PEO $1/T_1^{avg}$ increases dramatically above ~241 K, which is significantly above T_g determined from low-frequency measurements such as ellipsometry and DSC, while in PEO:$LiCF_3SO_3$ it increases above ~233 K. The change in $1/T_1^{avg}$ appears to result from activated $^8Li^+$ hopping that is facilitated by polymer motion. The onset temperature is higher than T_g measured by ellipsometry because β-NMR is sensitive to frequencies on the order of 41 MHz while ellipsometry measures the time-averaged film thickness. The change in T_g is known to be on the order of 3 K per decade of frequency, so the higher T_g is consistent with the higher frequency.

The temperature dependences of $1/T_1^{avg}$ in PEO and PEO:$LiCF_3SO_3$ are well described by the Arrhenius model (Figure 3). The data could be fit assuming a VFT model for τ, but this yielded an unrealistically low T_{VF} of 17 K compared with 177 K reported by Do et al., which is consistent with $T_{VF} \approx T_g - 50$ K.[12] We have concluded that the Arrhenius model is more appropriate and suggest that the hopping of Li^+ between neighboring sites is an activated process involving motion of the polymer but that long-range diffusion is dominated by the α process, which gives it the distinctive VFT temperature dependence.

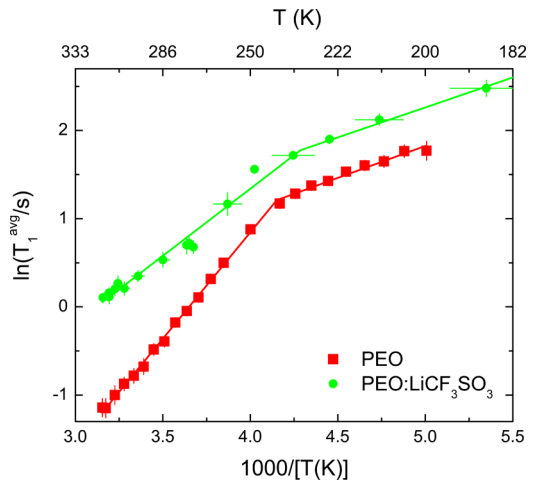

Figure 3. Arrhenius plot of $\ln(T_1^{avg}/s)$ versus inverse temperature for PEO and PEO with 30 wt % $LiCF_3SO_3$.

The maximum average E_A ($\alpha = 1$) was determined from the slope of $\ln(T_1/s)$ versus T^{-1} to be 20.1 ± 0.3 kJ/mol in PEO and 12.6 ± 0.6 kJ/mol in PEO:$LiCF_3SO_3$. The maximum value of E_A in PEO is lower than the value measured by Do et al. for the β-relaxation in PEO:LiTFSI. Baboul et al. studied Li^+ diffusion barriers in Li^+-$(diglyme)_2$ and $LiClO_4$-diglyme complexes and found the smallest Li^+ migration barriers for complexes with the highest coordination numbers.[28] The lower E_A in PEO:$LiCF_3SO_3$ then implies that Li^+ is coordinated to fewer oxygens in PEO than in PEO:$LiCF_3SO_3$, where powder X-ray diffraction has shown it is coordinated to five oxygen atoms (three ether oxygens and one from each of two adjacent $CF_3SO_3^-$ groups).[29]

We did not observe the T_1 minimum so we cannot calculate the absolute hop rate, but from the intercepts of the Arrhenius plot we estimate that τ_0^{-1} is at least 58 ± 16 times slower in PEO:$LiCF_3SO_3$ than in PEO, assuming the spin relaxation mechanism is identical in the two samples. $LiCF_3SO_3$ likely slows down hopping by blocking many of the EO cages surrounding $^8Li^+$ and slowing the polymer motions that assist Li^+ hopping, as evidenced by the larger T_g in PEO:$LiCF_3SO_3$. The larger τ_0^{-1} in PEO compared with PEO:$LiCF_3SO_3$ outweighs the larger E_A and results in faster Li^+ motion. At 300 K the Li^+ hop rate is 3.0 ± 1.1 times faster in PEO than PEO:$LiCF_3SO_3$.

β-NMR spectroscopy has been used to study the microscopic Li^+ diffusion in a SPE with an extremely low lithium ion concentration, which has allowed us to study the effect of adding a large concentration of an inorganic salt to the polymer. Hopping of Li^+ between neighboring sites is an activated process and is considerably slowed down by a large concentration of a lithium salt. Further measurements will be made on PEO samples with a wide range of $LiCF_3SO_3$ concentrations to better understand the effect of adding salt and optimize the conditions for maximum Li^+ diffusion. An oven is being designed to make it possible to observe the T_1 minimum and determine the absolute $^8Li^+$ hop rate.

AUTHOR INFORMATION

Corresponding Author

iain.mckenzie@triumf.ca

Notes

The authors declare no competing financial interest.

ACKNOWLEDGMENTS

We thank R. Abasalti and D. Vyas for technical assistance during the β-NMR experiments.

REFERENCES

(1) Ozawa, K., Ed. *Lithium Ion Rechargeable Batteries: Materials, Technology, and New Applications*; Wiley-VCH: Weinheim, 2009.
(2) Goodenough, J. B.; Kim, Y. *Chem. Mater.* **2010**, *22*, 587–603.
(3) Meyer, W. *Adv. Mater.* **1998**, *10*, 439–448.
(4) Nishimoto, A.; Watanabe, M.; Ikeda, Y.; Kojiya, S. *Electrochim. Acta* **1998**, *43*, 1177–1184.
(5) Müller-Plathe, F.; v. Gunsteren, W. F. *J. Chem. Phys.* **1995**, *103*, 4745–4756.
(6) Borodin, O.; Smith, G. D. *Macromolecules* **2006**, *39*, 1620–1629.
(7) Diddens, D.; Heuer, A.; Borodin, O. *Macromolecules* **2010**, *43*, 2028–2036.

(8) Berthier, C.; Gorecki, W.; Minier, M.; Armand, M. B.; Chabagno, J. M.; Rigaud, P. *Solid State Ionics* **1983**, *11*, 91−95.
(9) Gadjourova, Z.; Andreev, Y. G.; Tunstall, D. P.; Bruce, P. G. *Nature* **2001**, *412*, 520−523.
(10) Roach, D. J.; Dou, S.; Colby, R. H.; Mueller, K. T. *J. Chem. Phys.* **2012**, *136*, 014510.
(11) Do, C.; Lunkenheimer, P.; Diddens, D.; Götz, M.; Weiß, M.; Loidl, A.; Sun, X.-G.; Allgaier, J.; Ohl, M. *Phys. Rev. Lett.* **2013**, *111*, 018301.
(12) Ratner, M. A.; Johansson, P.; Shriver, D. F. *MRS Bull.* **2000**, *25*, 31−37.
(13) Salman, Z.; Ofer, O.; Radovic, M.; Hao, H.; Ben Shalom, M.; Chow, K. H.; Dagan, Y.; Hossain, M. D.; Levy, C. D. P.; MacFarlane, W. A.; Morris, G. M.; Patthey, L.; Pearson, M. R.; Saadaoui, H.; Schmitt, T.; Wang, D.; Kiefl, R. F. *Phys. Rev. Lett.* **2012**, *109*, 257207.
(14) Hossain, M. D.; Salman, Z.; Wang, D.; Chow, K. H.; Kreitzman, S.; Keeler, T. A.; Levy, C. D. P.; MacFarlane, W. A.; Miller, R. I.; Morris, G. D.; Parolin, T. J.; Pearson, M.; Saadaoui, H.; Kiefl, R. F. *Phys. Rev. B* **2009**, *79*, 144518.
(15) Heitjans, P. *Solid State Ionics* **1986**, *18−19*, 50−64.
(16) Heitjans, P.; Körblein, A.; Ackermann, H.; Dubbers, D.; Fujara, F.; Stöckmann, H.-J. *J. Phys. F: Met. Phys.* **1985**, *15*, 41−54.
(17) Freiländer, P.; Heitjans, P.; Ackermann, H.; Bader, B.; Kiese, G.; Schirmer, A.; Stöckmann, H.-J.; Van der Marel, C.; Magerl, A.; Zabel, H. *Z. Phys. Chem. Neue Fol.* **1987**, *151*, 93−101.
(18) Schirmer, A.; Heitjans, P.; Faber, W.; Clausen, D. *Solid State Ionics* **1992**, *53−56*, 426−430.
(19) Korblein, A.; Heitjans, P.; Stöckmann, H.-J.; Fujara, F.; Ackermann, H.; Buttler, W.; Dörr, K.; Grupp, H. *J. Phys. F: Met. Phys.* **1985**, *15*, 561−577.
(20) Salman, Z.; Kiefl, R. F.; Chow, K. H.; Hossain, M. D.; Keeler, T. A.; Kreitzman, S. R.; Levy, C. D. P.; Miller, R. I.; Parolin, T. J.; Pearson, M. R.; Saadaoui, H.; Schultz, J. D.; Smadella, M.; Wang, D.; MacFarlane, W. A. *Phys. Rev. Lett.* **2006**, *96*, 147601.
(21) Mattsson, J.; Forrest, J. A.; Krozer, A.; Södervall, U.; Wennerberg, A.; Torell, L. M. *Electrochim. Acta* **2000**, *45*, 1453−1461.
(22) Ziegler, J. http://www.srim.org/ (accessed May 14, 2014).
(23) Borgs, P.; Kehr, K. W.; Heitjans, P. *Phys. Rev. B* **1995**, *52*, 6668−6683.
(24) Andrew, E. R.; Tunstall, D. P. *Proc. Phys. Soc.* **1961**, *78*, 1−11.
(25) Bloembergen, N.; Purcell, E. M.; Pound, R. V. *Phys. Rev.* **1948**, *73*, 679−712.
(26) Kuhn, A.; Kunze, M.; Sreeraj, P.; Wiemhöfer, H.-D.; Thangaduraid, V.; Wilkening, M.; Heitjans, P. *Solid State Nucl. Magn. Reson.* **2012**, *42*, 2−8.
(27) Donoso, J. P.; Bonagamba, T. J.; Panepucci, H. C.; Oliveira, L. N.; Gorecki, W.; Berthier, C.; Armand, M. *J. Chem. Phys.* **1993**, *98*, 10026−10036.
(28) Baboul, A. G.; Redfern, P. C.; Sutjianto, A.; Curtiss, L. A. *J. Am. Chem. Soc.* **1999**, *121*, 7220−7227.
(29) Lightfoot, P.; Mehta, M. A.; Bruce, P. G. *Science* **1993**, *262*, 883−885.